Vortex mode decomposition of the topology-induced phase transitions in spin-orbit optics

Xiaohui Ling (凌晓辉),[1,*] Fuxin Guan,[2] Zan Zhang,[1] He-Xiu Xu,[3] Shiyi Xiao,[4,†] and Hailu Luo[5]

[1]*College of Physics and Electronic Engineering, Hengyang Normal University, Hengyang 421002, China*

[2]*Institute of Microscale Optoelectronics, Shenzhen University, Shenzhen 518060, China*

[3]*Air and Missile Defense College, Air Force Engineering University, Xi'an 710051, China*

[4]*Key Laboratory of Specialty Fiber Optics and Optical Access Networks, Joint International Research Laboratory of Specialty Fiber Optics and Advanced Communication, Shanghai Institute for Advanced Communication and Data Science, Shanghai University, Shanghai 200444, China*

[5]*Laboratory for Spin Photonics, School of Physics and Electronics, Hunan University, Changsha 410082, China*

(Received 19 July 2021; accepted 22 October 2021; published 2 November 2021)

The topology-induced phase transition (TPT) in spin-orbit optics refers to a process of topological transition from one kind of spin-orbit interaction (e.g., spin-controlled vortex generation) to another (e.g., photonic spin-Hall effect). However, it is not clear in the TPT how a light beam evolves from a vortex state with a topological charge of ± 2 to nonvortex states with spin-Hall shifts. Here, we examine the orbital angular momentum content (vortex harmonics) of a typical TPT process, i.e., the spin-orbit interactions of a light beam transmitted through an optically thin slab, based on vortex mode decomposition. It is found that the two kinds of spin-orbit interactions and the intermediate states can be described in a unified framework by considering the superposition and competition of three vortex modes with topological charges of 2, 1, and 0 (or -2, -1, and 0). These findings provide an alternative perspective for understanding the two spin-orbit interactions of light in a unified form and can be extended to the TPT-like processes in other physical systems.

DOI: 10.1103/PhysRevA.104.053504

I. INTRODUCTION

The spin-orbit interaction (SOI) of light manifests as the coupling and conversion between the spin angular momentum and the orbital angular momentum (OAM) [1–3]. There are two main SOI phenomena in optics, namely, spin-controllable vortex generation and photonic spin-Hall effect (for reviews, e.g., see Refs. [1–5]), which are, respectively, associated with the intrinsic and extrinsic OAM [3,6,7]. These two SOIs are widely found in many fundamental optical processes, such as light beam reflection and refraction at sharp interfaces [8–13], strong focusing [14–16], and passing through structured media [17–20], which make the SOI play an increasingly important role in nano-optics, plasmonics, and topological photonics [21–28].

The two SOIs of light seem to be apparently distinct phenomena. In some systems, however, there exists a transition from spin-dependent vortex generation (intrinsic OAM) to photonic spin-Hall effect (extrinsic OAM) in certain conditions, that is, from one topological state to another [29]. This effect is called a topology-induced phase transition (TPT) process which can be described in a unified form in terms of the competition and coupling of the intrinsic and extrinsic OAM. Typically, recently we have revealed that the TPT of a circular-polarization (CP) light beam reflected and refracted at sharp interfaces manifests as a topological transition from a spin-dependent vortex with a topological charge of 2 or -2, whose sign depends upon the handedness of the incident CP beam, in normal incidence to a nonvortex beam with a spin-Hall shift (with a topological charge of 0) at oblique incidence [29]. The underlying mechanism is attributed to the wave vector-dependent Pancharatnam-Berry phase, which consists of two competing and coupled parts, i.e., an azimuthal phase and a one-dimensional gradient phase. The former generates spin-dependent vortices, while the latter results in photonic spin-Hall effect. However, it is still not clear how the light beam evolves from a vortex with a topological charge of ± 2 to a nonvortex spin-Hall beam with a topological charge of 0.

In this paper, based on vortex mode decomposition [30–33], we examine the OAM contents in the TPT process and provide an alternative perspective to understand the two kinds of SOIs in a unified form. We find that a CP light beam scattered by an optical interface consists of a spin-reversed abnormal component and a spin-maintained normal one. A TPT process appears in the abnormal beam, which can be described as the competition and superposition of three vortex modes, including the states with topological charges of 2, 1, and 0 (or -2, -1, and 0). The averaged OAM per photon of the abnormal beam is fractional, which is a full quantum average over the three modes. With the physics fully uncovered, we finally extend the method to a TPT-like optical process, when a Gaussian beam is misaligned to pass through a fork hologram or a spiral phase plate.

II. THEORY AND MODEL

We consider the scattering of a CP beam of light by an optically thin, nonmagnetic slab placed in air which is

*xhling@hynu.edu.cn
†phxiao@shu.edu.cn

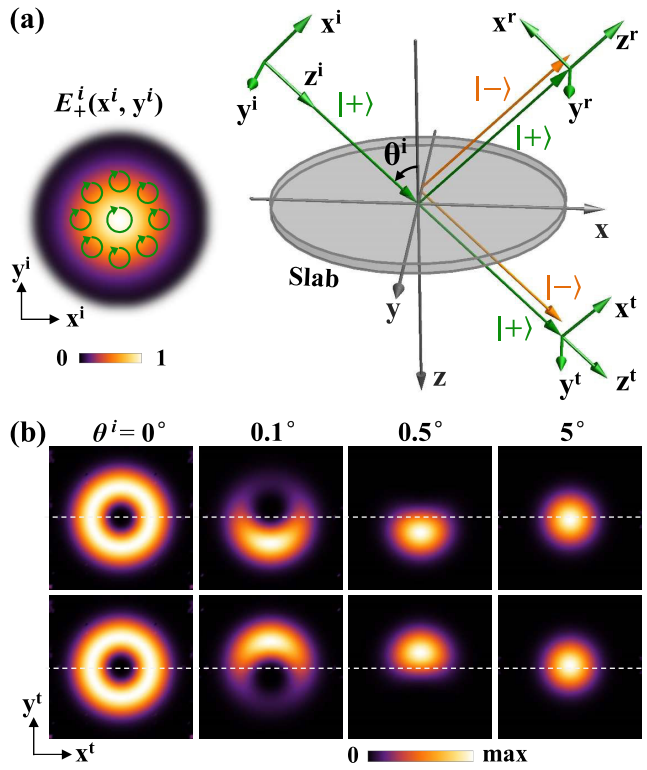

FIG. 1. Topology-induced phase transitions of light beam reflected and refracted from an optically thin slab. (a) Left: E-field and polarization distribution of the incident beam on its waist plane. Right: Schematic picture of a CP light beam reflected and refracted at an optically thin slab placed in air. Here $|+\rangle$ and $|-\rangle$ represent left- and right-handed CPs, respectively. (b) Transverse field patterns of the spin-reversal abnormal modes at different incident angles under left-handed (upper row) and right-handed (lower row) CP beam illumination.

homogeneous and isotropic with thickness h and dielectric permittivity ε. The beam is composed of many interfering plane waves with slightly different propagation directions, each of which has a different incident plane and Fresnel coefficients. We set $(x,\ y,\ z)$ as the laboratory Cartesian coordinate, (x^a, y^a, z^a) as local coordinate with z^a parallel to the beam propagation direction [Fig. 1(a)], and y and y^a point to the same direction, where the superscript $a = \{i, r, t\}$ labels incident, reflection, and transmission, respectively.

In the CP basis (spin basis), light beams in a transverse reference plane $z^a = d^a$ [Fig. 1(a)] can be written as

$$\mathbf{E}^a_\perp(\mathbf{r}^a) = \int d^2\mathbf{k}^a_\perp e^{i\mathbf{k}^a_\perp\cdot\mathbf{r}^a_\perp + ik^a_z z^a} \sum_{\sigma=+,-} U^a_\sigma(\mathbf{k}^a)\hat{\mathbf{V}}^a_\sigma, \qquad (1)$$

where $\mathbf{k}^a\cdot\mathbf{r}^a = \mathbf{k}^a_\perp\cdot\mathbf{r}^a_\perp + k^a_z z^a$, with $\mathbf{k}^a_\perp = k^a_x\hat{\mathbf{x}}^a + k^a_y\hat{\mathbf{y}}^a$ and $\mathbf{r}^a_\perp = x^a\hat{\mathbf{x}}^a + y^a\hat{\mathbf{y}}^a$ being transverse wave vector and position vector, respectively, $k^a_z = [(k^a)^2 - (k^a_\perp)^2]^{1/2}$ is the longitudinal wave vector component with k^a being the wave number, $\hat{\mathbf{V}}^a_\pm = (\hat{\mathbf{x}}^a \pm i\hat{\mathbf{y}}^a)/\sqrt{2}$ denote unit vectors of left- (+) and right-handed (−) CPs defined in the laboratory coordinate system, and $U^a_\pm(\mathbf{k}^a)$ dictate the transverse patterns of the ath beam in k space.

As the reflection and transmission share the same physics, we here only consider the transmission case. In our recent work [29], we have established a full-wave theory to connect the transmitted and incident beam, i.e.,

$$\begin{bmatrix} U^t_+(\mathbf{k}^t) \\ U^t_-(\mathbf{k}^t) \end{bmatrix} = \mathbf{M}^{(t)} \begin{bmatrix} U^i_+(\mathbf{k}^i) \\ U^i_-(\mathbf{k}^i) \end{bmatrix}, \qquad (2)$$

where the 2×2 Fresnel Jones matrix $\mathbf{M}^{(t)}$ can be written as

$$\mathbf{M}^{(t)} \approx \begin{bmatrix} t_{++}(\mathbf{k}_{||}) & t_{+-}(\mathbf{k}_{||})e^{-i\Phi^{\rm abn}_{\rm B}} \\ t_{-+}(\mathbf{k}_{||})e^{i\Phi^{\rm abn}_{\rm B}} & t_{--}(\mathbf{k}_{||}) \end{bmatrix}. \qquad (3)$$

Here, $t_{++}(\mathbf{k}_{||}) = t_{--}(\mathbf{k}_{||}) = [t_{\rm TM}(\mathbf{k}_{||}) + t_{\rm TE}(\mathbf{k}_{||})]/2$ and $t_{+-}(\mathbf{k}_{||}) = t_{-+}(\mathbf{k}_{||}) = [t_{\rm TM}(\mathbf{k}_{||}) - t_{\rm TE}(\mathbf{k}_{||})]/2$ are Fresnel transmission coefficients of waves in CP basis with tangential wave vector $\mathbf{k}_{||}$ defined in the laboratory coordinate system, and $\Phi^{\rm abn}_{\rm B} \approx 2\phi_{\mathbf{k}}\cos\theta^i$ is the wave vector-dependent Pancharatnam-Berry phase resulting from the spin reversal of the abnormal mode [29,34–36]. Such spin reversal comes from the effective "anisotropy" [i.e., $t_{+-} = (t_{\rm TM} - t_{\rm TE})/2 \neq 0$] of TM- and TE-polarized plane waves possessed by the interface under oblique incidence. Here, θ^i is the incident angle of the light beam, $\phi_k = \tan^{-1}(k_y/k_x)$ is the azimuthal angle of the incident planes of any noncentral plane wave with respect to that of the central one with $k_x = k^a_x\cos\theta^a + k^a_z\sin\theta^a$ and $k_y = k^a_y$ being the transverse wave vector components of arbitrary plane wave in the laboratory coordinates.

For an optically thin slab placed in free space, we have [37]

$$t_{\rm TM}(\mathbf{k}_{||}) = \left[\cos\left(k^{(2)}_z h\right) - \frac{i}{2}\left(\frac{k^{(1)}_z\varepsilon}{k^{(2)}_z} + \frac{k^{(2)}_z}{k^{(1)}_z\varepsilon}\right)\sin\left(k^{(2)}_z h\right)\right]^{-1}$$
$$t_{\rm TE}(\mathbf{k}_{||}) = \left[\cos\left(k^{(2)}_z h\right) - \frac{i}{2}\left(\frac{k^{(1)}_z}{k^{(2)}_z} + \frac{k^{(2)}_z}{k^{(1)}_z}\right)\sin\left(k^{(2)}_z h\right)\right]^{-1}, \qquad (4)$$

where $k^{(1)}_z = k^i\cos\vartheta^i$ and $k^{(2)}_z = k^S\cos\vartheta^S$ with $\vartheta^S = \sin^{-1}[\sin\vartheta^i/\sqrt{\varepsilon}]$ and $k^S = \sqrt{\varepsilon}k^i$. Here, $\vartheta^i = \sin^{-1}(k_{||}/k^i)$ is the incident angle of arbitrary plane waves with $k_{||} = (k^2_x + k^2_y)^{1/2}$.

As the incident beam is known, which is assumed as a CP Gaussian one in its waist plane [see Fig. 1(a)],

$$\mathbf{E}^i_+(\mathbf{r}^i_\perp)|_{z^i=d^i} = \exp[-(r^i_\perp/w_0)^2]\hat{\mathbf{V}}^i_+, \qquad (5)$$

whose angular spectrum $U^i_+(\mathbf{k}^i) = \frac{w_0^2}{2}\exp[-(k^i_\perp w_0)^2/4]$ and $U^i_-(\mathbf{k}^i) \equiv 0$ can be obtained by Fourier transforming the Gaussian term, where w_0 is the half-width of the beam waist. Inserting $U^i_\pm(\mathbf{k}^i)$ into Eq. (2) to get $U^t_\pm(\mathbf{k}^t)$, finally we obtain the real fields by putting $U^t_\pm(\mathbf{k}^t)$ into Eq. (1) as

$$E^t_+(\mathbf{r}^t_\perp) = \int d^2\mathrm{k}^t_\perp e^{i\mathbf{k}^t\cdot\mathbf{r}^t} t_{++}(\mathbf{k}_{||})U^i_+(\mathbf{k}^i)$$
$$E^t_-(\mathbf{r}^t_\perp) = \int d^2\mathrm{k}^t_\perp e^{i\mathbf{k}^t\cdot\mathbf{r}^t} t_{-+}(\mathbf{k}_{||})e^{i\Phi^{\rm abn}_{\rm B}(\mathbf{k}^t)}U^i_+(\mathbf{k}^i), \qquad (6)$$

which are, respectively, spin-maintained and spin-reversed beams. We refer to the spin-maintained beam as *normal* mode and the spin-reversed one as *abnormal* mode. The real intensity evolution of the abnormal mode shows a topological

transition from a vortex state in normal incidence to off-axis vortex states in small-angle incidence, and finally to nonvortex spin-Hall beams in large-angle incidence [29], as shown in Fig. 1(b). For interfaces or slabs composed of general materials (e.g., air and glass), the weight or conversion efficiency of the abnormal mode is extremely low ($|t_{-+,+-}| \ll |t_{++,--}|$); however, it is expected to be greatly enhanced by some specially designed metamaterials [29,38].

III. RESULTS AND DISCUSSION

A. Vortex mode decomposition

We now decompose the abnormal mode into a set of vortex harmonics. Since the Laguerre-Gaussian (LG) beams [39] form a complete, orthogonal, and infinite-dimensional basis for the solutions of wave equation in paraxial approximations, any field distribution can be decomposed into a superposition of that basis [30–33]. Two integers p and m are employed to describe the LG beams, where p is non-negative and determines the radial shape of beam, and m can be any integer values and determines the topological charge of the azimuthal phase. A higher-order LG beam ($m \neq 0$) contains an optical vortex with a topological charge m, and a well-defined OAM of $m\hbar$ per photon. To obtain the vortex and OAM content, we can calculate the projection of the abnormal mode into the LG basis with $p = 0$:

$$E_-^t(\mathbf{r}_\perp^t) = \sum_{l=-\infty}^{\infty} c_m E_{\mathrm{LG}_m}, \tag{7}$$

where

$$c_m = \frac{\iint E_{\mathrm{LG}_m}^* E_-^t dx^t dy^t}{\left(\iint |E_{\mathrm{LG}_m}|^2 dx^t dy^t\right)^{1/2} \left(\iint |E_-^t|^2 dx^t dy^t\right)^{1/2}} \tag{8}$$

is the normalized weight coefficient of the mth-order LG beam via calculating the inner product between the LG basis and the abnormal beam, and

$$\begin{aligned} E_{\mathrm{LG}_m} = {} & \frac{A_0}{w(z^t)}\left[\frac{\sqrt{2}r_\perp^t}{w(z^t)}\right]^{|m|} L^{|m|}\left[2\left(\frac{r_\perp^t}{w(z^t)}\right)^2\right] \\ & \times \exp\left[-\left(\frac{r_\perp^t}{w(z^t)}\right)^2\right] \exp\left[-i\left(k^t z^t - \frac{(k^t r_\perp^t)^2}{2R(z^t)}\right)\right] \\ & \times \exp\left[i(|m|+1)\xi(z^t)\right] \exp(im\varphi) \end{aligned} \tag{9}$$

is the E-field distribution of the LG mode. Here $A_0 = \sqrt{2\pi^{-1}|m|^{-1}}$ is a constant, $L^{|m|}$ is the associated Laguerre polynomial, $z_R = kw_0^2/2$ is the Rayleigh range, $w(z^t) = w_0\sqrt{1+(z^t/z_R)^2}$ is the beam waist half-width at distance z^t, $R(z^t) = z^t + z_R^2/z^t$ is the curvature radius of wave front, and $\xi(z^t) = \tan^{-1}(z^t/z_R)$ is the Gouy phase. In the actual calculation of Eq. (8), we take a finite number of points to calculate the integrals numerically. And, c_m is a complex constant, which satisfies $\sum |c_m|^2 = 1$.

We now analyze the vortex harmonics constituent of the abnormal mode of the transmitted beam under a left-handed CP illumination. The abnormal mode is composed of three harmonics, i.e., $m = 2, 1, 0$ [see Fig. 2(a)]. For the incidence of a right-handed CP beam, the constituent harmonics are

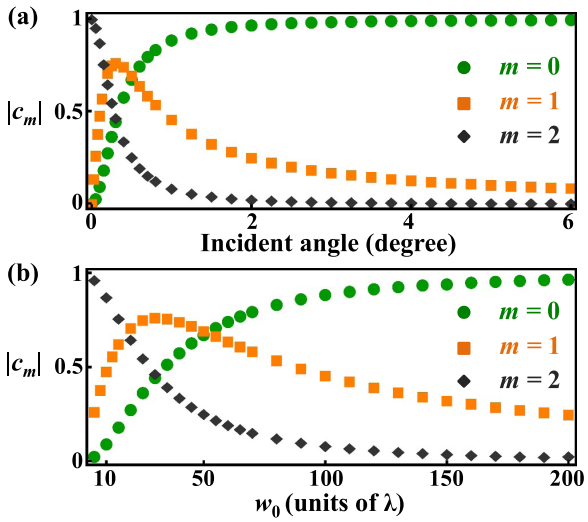

FIG. 2. Vortex mode weight of the abnormal modes. (a) Weight coefficients of the vortex harmonics varying against incident angle with beamwidth $w_0 = 50\ \lambda$. (b) Weight coefficients of the vortex harmonics vs beamwidth with $\theta^i = 0.5^\circ$. Here we set $\lambda = 1$, $h = 0.5\ \lambda$, and $z^t = 10\ \lambda$.

$m = -2, -1, 0$. At normal incidence, there is only $m = 2$ vortex harmonics, namely a perfect vortex. When the incident angle is slightly larger, harmonics $m = 1$ and 0 appear, and compete with $m = 2$. Their interference and superposition result in crescent-shaped intensity patterns [see Fig. 1(b)]. When the incident angle further increases, the abnormal mode is dominated by the harmonics $m = 0$. And, the high-order harmonics $m = 1$ and 2 become insignificant. Here, we have $\arg(c_0) \approx -\pi/2$, $\arg(c_1) \approx 0$, and $\arg(c_2) \approx \pi/2$ for all incident angles. The beam half-width w_0 is also an important parameter for controlling the TPT [29]. We plot the mode constituent versus w_0 in Fig. 2(b). As w_0 increases, the evolution of the weight coefficients of each mode has a similar behavior as those of increasing the incident angle in Fig. 2(a).

To intuitively illustrate the vortex mode superposition, we plot the magnitude, real, and imaginary parts of the constituent harmonics ($c_m E_{\mathrm{LG}_m}$), respectively (Fig. 3). It is evident that when the real part of the $m = 1$ mode is added to the $m = 2$ mode (real of the $m = 0$ mode is vanishing), the centroid of the superimposed beam has a shift in the $-y^t$ direction. Similarly, if the imaginary part of the $m = 1$ mode is added to that of $m = 0$ or 2 modes, the centroid of the superimposed beam will shift to the $-y^t$ direction. Hence, the existence of $m = 1$ mode is the origin of the beam centroid shift. The existence of the $m = 2$ mode can deform the beam profile.

B. Physical origin of the vortex mode generation

To further reveal the underlying physics of vortex mode generation with an easily accessible picture, we now explore the wave vector-dependent Pancharatnam-Berry phase $\Phi_{\mathrm{B}}^{\mathrm{abn}} \approx 2\phi_{\mathbf{k}} \cos\theta^i$ of the abnormal mode [Eq. (3)] with reasonable approximations. First, for normal incidence ($\theta^i = 0$), we can obtain $\Phi_{\mathrm{B}}^{\mathrm{abn}} \equiv 2\varphi$ without employing any approximation, which is a vortex phase with topological charge of 2. For oblique incidence cases still in the TPT region,

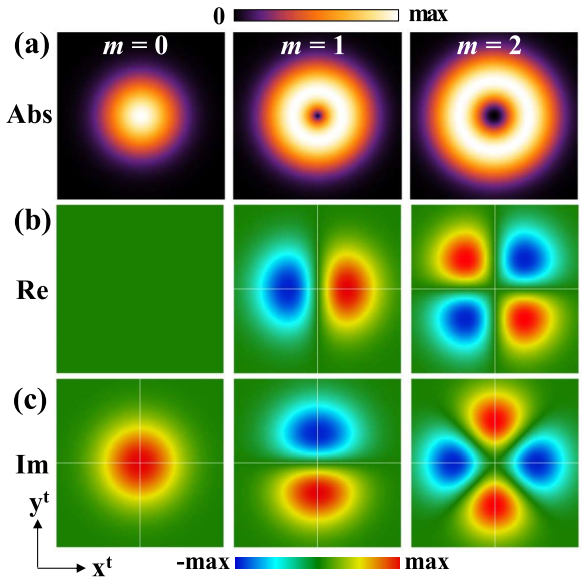

FIG. 3. Amplitudes (a), real (b), and imaginary (c) parts of the constituent vortex harmonics ($c_m E_{\mathrm{LG}_m}$).

that is, θ^i is within a few degrees, we approximately have $\Phi_{\mathrm{B}}^{\mathrm{abn}} \approx 2\phi_{\mathbf{k}} \cos\theta^i \approx 2\phi_{\mathbf{k}}$ and arrive at

$$e^{i2\Phi_{\mathrm{B}}^{\mathrm{abn}}} \approx \frac{\left[\left(k_x^i+\alpha\right)+ik_y\right]^2}{\left(k_x^i+\alpha\right)^2+k_y^2} = \frac{(k_\perp^i)^2 e^{i2\varphi}+2\alpha k_\perp^i e^{i\varphi}+\alpha^2}{\left(k_x^i+\alpha\right)^2+k_y^2}, \tag{10}$$

where $\alpha = k_z^i \sin\theta^i \approx k^i \sin\theta^i$. Equation (10) represents an asymmetric vortex in k space with its singular point shifting $-\alpha$ to the k_x^i direction. Because of the correspondence between the real space and k space, the real-field patterns exhibit y-direction shifts [Fig. 1(b)]. In this case, the phase factor of the abnormal mode can be decomposed into three vortex phase terms with topological charge of 2, 1, and 0, respectively. Therefore, the theoretical analysis also verifies the above numerical calculation. At the same time, we can clearly know from Eq. (10) that the proportion of the three vortex modes depends on the incident angle θ^i and $k_\perp^i$. The latter helps us to identify an important parameter w_0 to control the weight of the vortex modes because the half-width of the angular spectrum ($k_\perp^{\mathrm{HW}}$) of the beam is inversely proportion to w_0.

C. Calculation of OAM

To further verify the vortex mode decomposition method, we now consider the OAM of the abnormal beam. In fact, from the weighted coefficients of the vortex modes, we can directly compute the averaged OAM per photon in the z^t direction as [30]

$$\bar{L} = \sum m|c_m|^2, \tag{11}$$

which is a full quantum average over all the vortex constituents. The averaged OAM per photon can also be calculated by [29]

$$\bar{L} = \langle \mathbf{E}|-i\left(x^t\partial_{y^t} - y^t\partial_{x^t}\right)|\mathbf{E}\rangle / \langle \mathbf{E}|\mathbf{E}\rangle, \tag{12}$$

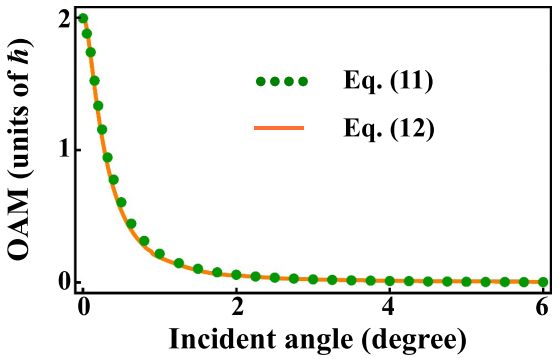

FIG. 4. Averaged OAM per photon of the abnormal mode calculated by two different methods. Here $h = 0.5\ \lambda$, $w_0 = 50\ \lambda$, and $z^t = 10\ \lambda$.

where $\mathbf{E}$ contains the two Cartesian components of the abnormal mode $E_-^t(\mathbf{r}_\perp^t)\hat{\mathbf{V}}_-^t$. The results of the averaged OAM per photon calculated by Eqs. (11) and (12), respectively, agree well with each other, as shown in Fig. 4, which indicates that the total OAM is fractional and proves the vortex mode decomposition method.

IV. EXTENSIONS

We now extend the above method and discussion to other optical systems. In fact, the crescent-shaped intensity patterns in the TPT process [see Fig. 1(b)] are very akin to the asymmetric Gaussian optical vortex [Fig. 5(a)] resulting from the misalignment of the Gaussian beam and the centers of the fork hologram or the spiral phase plate [40–43], which are readily observed in experiments. Strictly speaking, the diffraction of a shifted Gaussian beam by an amplitude fork hologram is very complex. Here we only consider a simple model situation and assume that the propagation distance is far less than the Rayleigh range; then, the field distribution of the transmitted

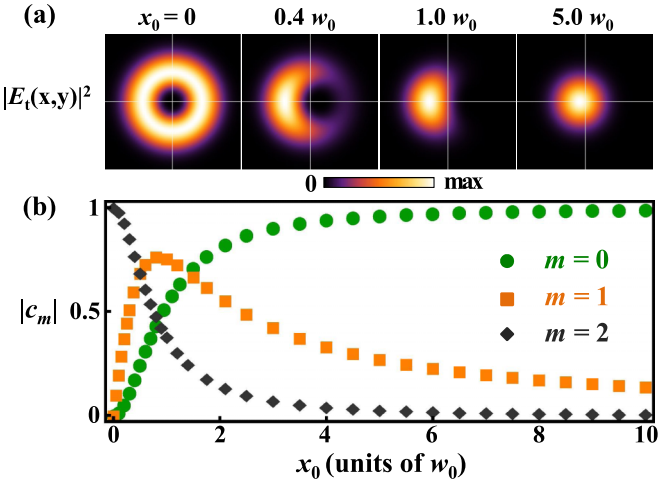

FIG. 5. Extensions of the vortex mode decomposition to asymmetric Gaussian optical vortex. (a) Intensity patterns for different misalignment distance x_0. (b) Weight coefficients of the vortex harmonics varying against x_0 with beamwidth $w_0 = 50\ \lambda$.

beam can be expressed as

$$E_t(x, y) \propto [(x - x_0) + i\mathrm{sgn}(n)y]^{|n|} \exp\left(-\frac{x^2 + y^2}{w_0^2}\right), \quad (13)$$

where x_0 is the misalignment distance in the x direction and n is the topological charge of the vortex produced by the alignment of the Gaussian beam and the centers of the fork hologram. Corresponding to the previous discussion, let $n = 2$, we get

$$E_t(x, y) = \left(r^2 e^{i2\varphi} - 2x_0 r e^{i\varphi} + x_0^2\right) \exp\left(-\frac{r^2}{w_0^2}\right). \quad (14)$$

Here $r = (x^2 + y^2)^{1/2}$. Unambiguously, the transmitted beam is also composed of three vortex harmonics, whose evolution behavior [see Fig. 5(b)] is the same as that in Fig. 2. The value of n can be any nonzero integer as long as the topological geometry of the fork hologram or the spiral phase plate is properly designed. However, for the model of reflection and refraction of a beam at an interface discussed in this paper, the maximum order of the vortex mode is 2 due to the properties of the wave vector-dependent Pancharatnam-Berry phase [29,35]. If n is a positive integer, the misalignment generates $n + 1$ vortex modes with topological charge of $n, n-1, \ldots,$ and 0, respectively; while n is a negative integer, then it generates $n + 1$ vortex modes with topological charge of $n, n + 1, \ldots,$ and 0, respectively.

V. CONCLUSIONS

In summary, based on the vortex mode decomposition, we have revealed that the TPT process in beam reflection and refraction at a sharp interface can be described by the competition and superposition of three vortex harmonics with topological charges of $m = 2$, 1, and 0 (or -2, -1, and 0). Quantitative calculation shows that the complete quantum average of the vortex mode coefficients equals to the averaged OAM per photon, which indicates that the vortex mode decomposition provides an effective way to describe the TPT in spin-orbit photonics. Since in other SOI systems, such as a q plates [18,32], and some non-SOI systems, such as fork holograms and spiral phase plates [40–43], similar TPT phenomena can also occur, our findings can be generalized to these systems.

ACKNOWLEDGMENTS

We acknowledge support from the National Natural Science Foundation of China (Grants No. 11874142 and No. 11604087), the National Key Research and Development Program of China (Grant No. 2017YFA0700202), and Laboratory of Optoelectronic Control and Detection Technology of the institution of higher learning of Hunan Province.

[1] K. Y. Bliokh, F. J. Rodríguez-Fortuño, F. Nori, and A. V. Zayats, Nat. Photon. **9**, 796 (2015).
[2] A. Aiello, P. Banzer, M. Neugebauer, and G. Leuchs, Nat. Photon. **9**, 789 (2015).
[3] K. Y. Bliokh and F. Nori, Phys. Rep. **592**, 1 (2015).
[4] S. Xiao, J. Wang, F. Liu, S. Zhang, X. Yin, and J. Li, Nanophotonics **6**, 215 (2017).
[5] X. Ling, X. Zhou, K. Huang, Y. Liu, C.-W. Qiu, H. Luo, and S. Wen, Rep. Prog. Phys. **80**, 066401 (2017).
[6] A. T. O'Neil, I. MacVicar, L. Allen, and M. J. Padgett, Phys. Rev. Lett. **88**, 053601 (2002).
[7] A. Bekshaev, K. Y. Bliokh, and M. Soskin, J. Opt. A **13**, 053001 (2011).
[8] M. Onoda, S. Murakami, and N. Nagaosa, Phys. Rev. Lett. **93**, 083901 (2004).
[9] K. Y. Bliokh and Y. P. Bliokh, Phys. Rev. Lett. **96**, 073903 (2006).
[10] O. Hosten and P. Kwiat, Science **319**, 787 (2008).
[11] Y. Qin, Y. Li, H. He, and Q. Gong, Opt. Lett. **34**, 2551 (2009).
[12] M. Yavorsky and E. Brasselet, Opt. Lett. **37**, 3810 (2012).
[13] A. Ciattoni, A. Marini, and C. Rizza, Phys. Rev. Lett. **118**, 104301 (2017).
[14] Y. Zhao, J. S. Edgar, G. D. M. Jeffries, D. McGloin, and D. T. Chiu, Phys. Rev. Lett. **99**, 073901 (2007).
[15] K. Y. Bliokh, E. A. Ostrovskaya, M. A. Alonso, O. G. Rodríguez-Herrera, D. Lara, and C. Dainty, Opt. Express **19**, 26132 (2011).
[16] V. V. Kotlyar, A. G. Nalimov, A. A. Kovalev, A. P. Porfirev, and S. S. Stafeev, Phys. Rev. A **102**, 033502 (2020).
[17] Z. Bomzon, V. Kleiner, and E. Hasman, Opt. Lett. **26**, 1424 (2001).
[18] L. Marrucci, C. Manzo, and D. Paparo, Phys. Rev. Lett. **96**, 163905 (2006).
[19] E. Karimi, S. A. Schulz, I. De Leon, H. Qassim, J. Upham, and R. W. Boyd, Light Sci. Appl. **3**, e167 (2014).
[20] R. C. Devlin, A. Ambrosio, N. A. Rubin, J. P. B. Mueller, and F. Capasso, Science **358**, 896 (2017).
[21] N. Shitrit, I. Yulevich, E. Maguid, D. Ozeri, D. Veksler, V. Kleiner, and E. Hasman, Science **340**, 724 (2013).
[22] L. Huang, X. Chen, B. Bai, Q. Tan, G. Jin, T. Zentgraf, and S. Zhang, Light: Sci. Appl. **2**, e70 (2013).
[23] Q. Guo, W. Gao, J. Chen, Y. Liu, and S. Zhang, Phys. Rev. Lett. **115**, 067402 (2015).
[24] D. Pan, H. Wei, L. Gao, and H. Xu, Phys. Rev. Lett. **117**, 166803 (2016).
[25] E. Maguid, M. Yannai, A. Faerman, I. Yulevich, V. Kleiner, and E. Hasman, Science **358**, 1411 (2017).
[26] J. Zhou, H. Qian, C. Chen, J. Zhao, G. Li, Q. Wu, H. Luo, S. Wen, and Z. Liu, Proc. Natl. Acad. Sci. USA **116**, 11137 (2019).
[27] S. Fu, C. Guo, G. Liu, Y. Li, H. Yin, Z. Li, and Z. Chen, Phys. Rev. Lett. **123**, 243904 (2019).
[28] L. Du, Z. Xie, G. Si, A. Yang, C. Li, J. Lin, G. Li, H. Wang, and X. Yuan, ACS Photon. **6**, 1840 (2019).
[29] X. Ling, F. Guan, X. Cai, S. Ma, H.-X. Xu, Q. He, S. Xiao, and L. Zhou, Laser Photon. Rev. **15**, 2000492 (2021).

[30] G. Molina-Terriza, J. P. Torres, and L. Torner, Phys. Rev. Lett. **88**, 013601 (2001).
[31] M. V. Vasnetsov, V. A. Pas' Ko, and M. S. Soskin, New J. Phys. **7**, 46 (2005).
[32] A. D'Errico, R. D'Amelio, B. Piccirillo, F. Cardano, and L. Marrucci, Optica **4**, 1350 (2017).
[33] Y. Yang, Q. Zhao, L. Liu, Y. Liu, C. Rosales-Guzmán, and C.-W. Qiu, Phys. Rev. Appl. **12**, 064007 (2019).
[34] L.-K. Shi and J. C. W. Song, Phys. Rev. B **100**, 201405(R) (2019).
[35] X. Ling, H. Luo, F. Guan, X. Zhou, H. Luo, and L. Zhou, Opt. Express **28**, 27258 (2020).
[36] W. Zhu, H. Zheng, Y. Zhong, J. Yu, and Z. Chen, Phys. Rev. Lett. **126**, 083901 (2021).
[37] M. Born and E. Wolf, *Principles of Optics* (Cambridge University Press, Cambridge, UK, 1999).
[38] X. Ling, W. Xiao, S. Chen, X. Zhou, H. Luo, and L. Zhou, Phys. Rev. A **103**, 033515 (2021).
[39] L. Allen, M. W. Beijersbergen, R. J. C. Spreeuw, and J. P. Woerdman, Phys. Rev. A **45**, 8185 (1992).
[40] A. Ya. Bekshaev and A. I. Karamoch, Opt. Commun. **281**, 3597 (2008).
[41] A. Ya. Bekshaev and S. V. Sviridova, Opt. Commun. **283**, 4866 (2010).
[42] F. Li, Y.-S. Jiang, J. Ou, and H. Tang, Acta Physica Sinica **60**, 084201 (2011).
[43] V. V. Kotlyar, A. A. Kovalev, and A. P. Porfirev, Opt. Lett. **42**, 139 (2017).